which was used as pulse duplicator of the endurance test had to be exchanged because a crack occurred in the diaphragm [11]. Additionally, breakage of the diaphragm of a pneumatic pulsatile VAD was also reported at the 17th Japanese association for clinical ventricular assist systems, held in 2011. Thus, diaphragms or sacs made from flexible materials have the possibility of fatigue or fracture after long-term continuous operation. The evaluation of VADs may possibly be influenced when diaphragm breakage in the test equipment occurs during the process of the durability test. Therefore, the test equipment requires durability and stability that can be continually driven for long periods of time without device failure.

In addition, the development of VADs for children has been promoted in recent years [14–17]. It is necessary to evaluate these devices on each target specification because the circulatory conditions of the living human body are not uniform. Therefore, it is necessary that the test equipment is versatile and can simulate various circulatory conditions for a range of devices.

There is an industrial pulsatile pump which has an active filling mechanism as a pulsatile pump with durability. However, since this industrial pulsatile pump is a constant volume pump, there is no compliance in this pulsatile pump. It is difficult to simulate a ventricle with compliance using this pulsatile pump. Therefore, we recently proposed giving compliance to the industrial pulsatile pump with durability by connecting a closed chamber to the pulsatile pump in order to simulate a circulatory condition similar to that of hemodynamics in the living human body. In addition, various circulatory conditions can be quantitatively simulated by varying the compliance of the pulsatile pump. Thus, we developed a novel endurance test system which can simulate various circulatory conditions with durability and stability by applying the industrial pulsatile pump and the closed chamber. The present study describes the evaluation of the reproduction of pulsatility due to the effect of the closed chamber connected to the pulsatile pump and an investigation into the range of reproducible circulatory conditions by the developed endurance test system. In addition, a long-term continuous operation experiment was carried out in order to assess the durability and stability of the endurance test system.

Materials and methods

Description of endurance test system

The newly developed endurance test system for evaluating the durability and reliability of VADs consists of a circulation circuit, a measurement device, several sensors and a control device. The system specifications are shown in Table 1. Figures 1 and 2 show a schematic drawing and an image of the circulation circuit. The circulation circuit consists of the pulsatile pump with a small closed chamber (SCC), a closed chamber, a reservoir, an electromagnetic flow meter and an electromagnetic proportional valve. Each component is connected to pipes by a ferrule that is simple to maintain. The pipes are made of stainless steel and are 35.7 mm inner diameter. The pulsatile pump (AXA-120; Iwaki Co., Ltd., Tokyo, Japan), which approximates the left ventricle (LV), has an active diaphragm-type filling mechanism. The pulsatile pump consists of a diaphragm, a drive shaft and a motor as a driving source. The drive shaft directly connects the diaphragm and the motor, and the position of the diaphragm creates a back and forth motion in the shape of a sine wave by the motor. The pulsatile pump has a variable heart rate (HR) and stroke length (SL); HR can be regulated from 0 to 120 bpm; and SL, which can change the stroke volume of the pulsatile pump, can be adjusted quantitatively between 0 and 100 %, with 100 % SL being about 84 ml in the stroke volume, and 0 % SL being 0 ml in the stroke volume. Also, the pulsatile pump has a fixed systole ratio of 50 %. The SCC, which is small in volume compared with the closed chamber, is connected to the pulsatile pump and contains a mixture of air and fluid. The compliance of the pulsatile pump can be adjusted by changing the air volume in the SCC. The duckbill valves are made of synthetic rubber and are mounted as inlet and outlet valves in the pulsatile pump. The working fluid is then circulated in one direction. The closed chamber approximates the aorta (Ao) and contains a mixture of air and fluid, with the compliance of the Ao adjusted by air volume. The reservoir, which approximates the left atrium (LA), is opened to the atmosphere in order to remove the effect of arterial pulsatility and to give an established pressure; and adjusting the water level alters the pre-load of the pulsatile pump. The electromagnetic proportional valve (RDH124-2; KITZ, Chiba, Japan), which approximates the peripheral resistance (PR), is connected to change the fluid resistance of the circulation circuit. The fluid resistance can be changed quantitatively by varying a gate opening of the electromagnetic proportional valve from 0 to 100 %; and 100 % gate opening is fully opening and 0 % gate opening closes almost completely. Test objects such as VADs are connected to the

Table 1 Endurance test system specifications

Flow range (l/min)	0 to 10
Pressure range (mmHg)	−200 to 300
Heart rate range (bpm)	0 to 120
Wetted material	SUS304, PVC, synthetic rubber
Size ($W \times D \times H$) (mm)	1000 × 1000 × 1500
Weight (kg)	250

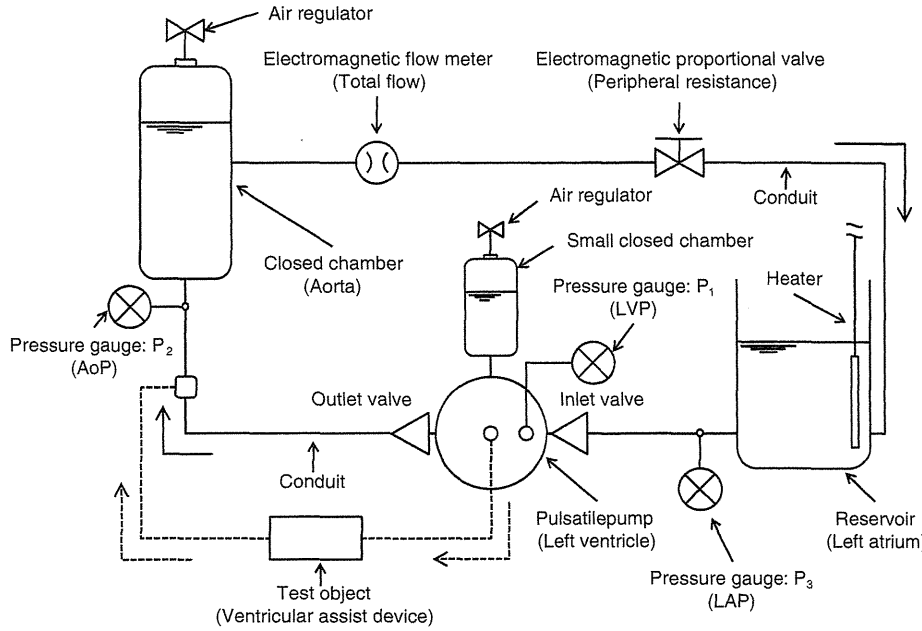

Fig. 1 Schematic diagram of the circulation circuit

pulsatile pump upstream of the closed chamber, and its durability and reliability can then be evaluated. The features of the developed circulation circuit are as follows: (1) the components of this circulation circuit consist of optimized industrial devices, with rigid piping made from stainless steel being used, thereby ensuring durability for the long-term operation of VADs; (2) the pulsatile pump can vary HR and stroke volume, as well as its compliance using the SCC, which ensures that the endurance test system can quantitatively simulate various circulatory conditions.

In terms of sensors, pressure transducers (PA-500; Nidec Copal Electronics Corporation, Tokyo, Japan) were attached to measure the pressures generated by the circulation circuit, and the range of these pressure gauges was between −200 and 300 mmHg. Pressure measurements for parts P1, P2 and P3 of the circulation circuit in Fig. 1 were considered to approximate left ventricle pressure (LVP), aortic pressure (AoP) and left atrium pressure (LAP), respectively. The electromagnetic flow meter (MGS11U; Azbil, Tokyo, Japan) was attached between the closed chamber and the electromagnetic proportional valve in order to measure total flow (TF). A heater and a thermocouple were installed in the reservoir and could be controlled such that the working fluid reaches a preset temperature. The pressure sensors were selected in consideration of the range of pressure in the living human body. The electromagnetic flow meter, heater and the thermocouple were selected from industrial devices in consideration of durability.

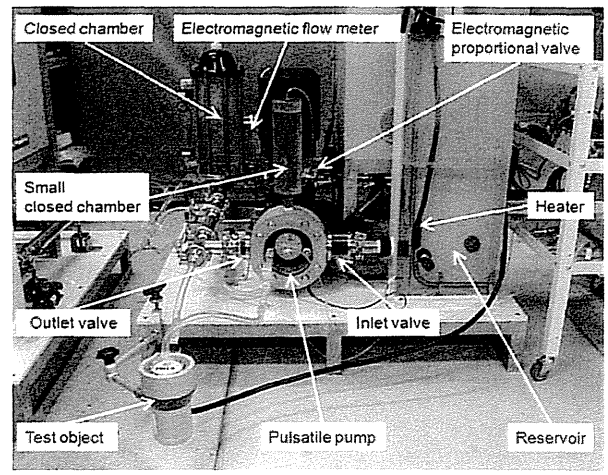

Fig. 2 Image of the circulation circuit

In terms of control, the endurance test system can regulate the HR and SL of the pulsatile pump, and the resistance of the electromagnetic proportional valve electronically using a liquid crystal display controller (GT1150-QLBD; Mitsubishi Electric Corporation, Tokyo, Japan). Moreover, for the prolonged test, automatic operation is possible for a life pattern (awake, sleep, exercise, etc.) which incorporates the circulatory conditions and time schedule, which are set up beforehand.

For measurement, a multi-unit PC data acquisition system (NR-600; Keyence, Osaka, Japan) was used. With 2 GB of storage, approximately 1 month of data collection

is possible for a maximum of eight channels at a sampling frequency of 100 Hz.

Specific targets of the endurance test system

The pre-load and after-load of VADs are LVP and AoP at the circulation circuit. LVP and AoP in the adult condition are reported as 120–0 mmHg, 120–80 mmHg [18]. In addition, it is reported that the ranges of AoP and HR in children (0–18 years) are approximately 120–60 mmHg and 80–140 bpm [19, 20]. Therefore, in order to verify whether it is possible to observe the pulsatile load equivalent to a living human body in our circulation circuit, we defined the pressure values of LVP and AoP for the cardiac cycle, the TF and HR values in normal adults and children (Table 2).

According to the guidelines of the Ministry of Economy, Trade and Industry of Japan, endurance testing for at least 6 months or more must be carried out in preclinical studies in Japan [21]. In this article, a target for the period of durability test of our system decided on 6 months.

Effect of SCC and reproduction of pulsatility of pressure wave forms

In this study, the SCC was added in order to vary the compliance of the pulsatile pump. First, static characteristics between the pressure and the fluid volume in the SCC were investigated in order to evaluate the compliance in each air volume of SCC. Figure 3a shows a measuring method of static characteristics of SCC. Experiments were conducted using the SCC alone. The SCC was filled with fluid and constant air volume (air volume of SCC = 250, 500 and 750 ml). Then the fluid was injected into the SCC at 10 ml intervals using a syringe quantitatively and the pressures of fluid inside the SCC were measured using the pressure gauge. Figure 3b shows a static relation between the pressure of fluid inside the SCC and the injected fluid volume in each air volume of SCC, and an elastance (reciprocal of the compliance) was found from each characteristic (Table 3). It is reported that the elastance of the living human body is approximately 3 mmHg/ml [22]. Therefore, the initial air volume of SCC was decided on 250 ml.

Table 2 Physiological conditions

	Adults	Children
LVP (mmHg)	120–0	120–0
AoP (mmHg)	120–80	120–60
Mean AoP (mmHg)	100	90
HR (bpm)	70	120
Total flow (l/min)	5	3

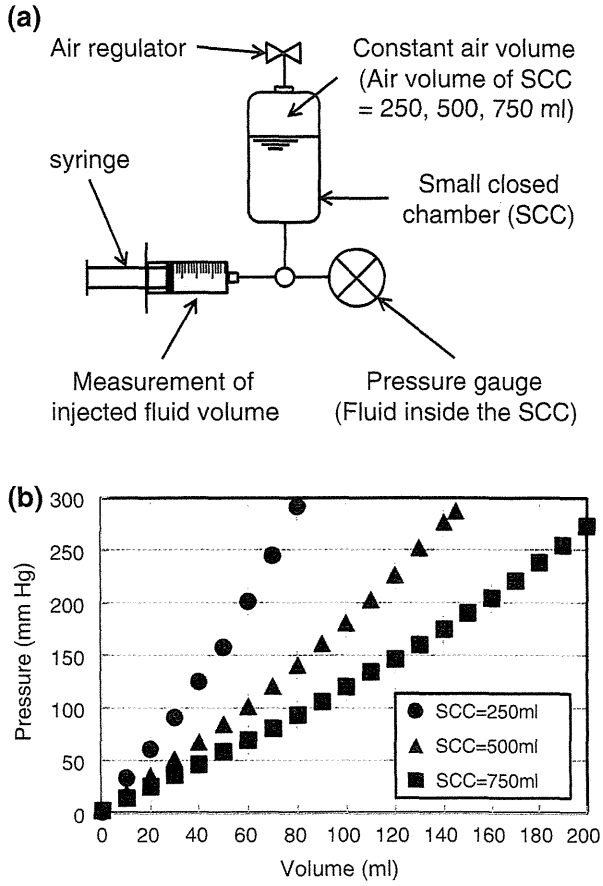

Fig. 3 **a** Measuring method of static characteristics of SCC. **b** Static relation between the pressure of fluid inside the SCC and the injected fluid volume in each air volume of SCC

Table 3 Elastance values in each air volume of SCC

Air volume of SCC (ml)	Elastance (mmHg/ml)
250	3.58
500	1.96
750	1.37

Next, in terms of the effects of SCC, the relationship between the air volume in SCC and output of the pulsatile pump in the circulation circuit were examined. Experiments were conducted using the circulation circuit alone without the test object. As an initial condition for the circulation circuit, the air volume of SCC, HR and SL of the pulsatile pump were set at 250 ml, 70 bpm and 100 %. After the circulation circuit was initiated, the electromagnetic proportional valve, the air volume in the closed chamber and the water level of the reservoir were regulated such that the AoP and LAP were set at 120–80 mm Hg (mean AoP = 100 mmHg) and 20 mmHg, respectively,

while operating the circulation circuit, and the air volume of closed chamber was maintained constant. Here, the negative pressure of LVP was indicated in the preliminary test. Therefore, LAP was set at 20 mmHg in order to reduce the negative pressure of LVP as much as possible. After operation of the circulation circuit stabilized, the air volume of SCC was regulated at 50 ml intervals from 0 to 750 ml while operating the circulation circuit, and the maximum and minimum values for LVP (max LVP and min LVP), mean AoP and mean TF were measured. Particularly, the wave forms for LVP and AoP, and the mean value of TF were compared when the air volume of SCC was adjusted to 0, 250 and 500 ml. Here, these conditions of air volume of SCC were decided in order to compare eliminated and increased compliance against 250 ml.

Evaluation of the range of reproducible circulatory conditions

The range of reproducible circulatory conditions was examined as a fundamental performance of the circulation circuit. The electromagnetic proportional valve, the air volume in the closed chamber and the water level of the reservoir were regulated such that AoP and LAP were set to 120–80 mmHg (mean AoP = 100 mmHg) and 20 mmHg, respectively, while operating the circulation circuit when the air volume of SCC was 0, 250 and 500 ml. Under these conditions, the fixed SL was 100 %. The fluid resistance of the circulation circuit was changed by varying the gate opening of electromagnetic proportional valve from 100 % to 20–60 % (pressure measurement range is under 300 mmHg) in order to vary the TF in each given HR for each air volume of SCC. Here, since the fluid resistance of the electromagnetic proportional valve was not linear with respect to the gate opening, the gate opening was therefore regulated at 20 % intervals from 100 to 60 % and was regulated at 5–10 % intervals under 60 %. In addition, the max LVP, min LVP, mean AoP and mean TF were recorded, and the same experiments as previously described were conducted when the pulsatile pump SL was adjusted to 50, 75 and 100 %. Under these conditions, the fixed air volume of SCC was 250 ml. The air volumes of SCC and SL were readjusted while stopping the circulation circuit.

Long-term continuous operation experiment

A long-term continuous operation experiment was conducted for 6 months in order to evaluate the durability and stability of the endurance test system. The experiment was conducted under fixed conditions, and the circulatory conditions and control parameters were as shown in Table 4. Several factors, including industrial device failure, fluid leakage and changes in pressure wave form, which are attributed to long-term continuous operation, were evaluated.

Table 4 Parameters for long-term operation

Air volume of SCC (ml)	250
HR (bpm)	70
AoP (mmHg)	120–80 (100)
LAP (mmHg)	20
Total flow (l/min)	4.5
PR (%)	44

Experimental conditions

The viscosity of the working fluid had a possibility of changing due to evaporation during the experiments because the reservoir used in our circulation circuit was open to the atmosphere. Therefore, in all experiments, tap water (viscosity, 0.001 Pa s) at 37 °C was used as the working fluid.

In terms of data acquisition, in all experiments, the sampling frequencies for the three pressure channels and the TF and temperature of the working fluid channels were set at 100 and 10 Hz, respectively.

Results

Effect of SCC and reproduction of pulsatility of pressure wave forms

The characteristic max and min LVP, mean AoP, and mean TF when the SCC air volume was varied from 0 to 750 ml are shown in Fig. 4. Then the LAP in each condition was 20 mmHg. The max and min LVP, mean AoP, and mean TF showed nonlinear characteristics against the air volume in SCC, and each absolute value decreased with increasing air volume in SCC. LVP and AoP wave forms when the air volume of SCC was 0, 250 and 500 ml are shown in Fig. 5. The max and min LVP, as well as pulse pressure, decreased when the air volume of SCC was increased from 0 to 250 or 500 ml. The mean and pulse pressure of AoP also decreased. The mean TFs at SCC air volumes of 0, 250 and 500 ml were 5.6, 4.4 and 3.8 l/min, respectively. Although pressure wave forms with a spike were observed when the air volume of SCC was 0 ml, there was no spike in the wave forms when the air volume of SCC was 250 and 500 ml. The defined pressure ranges were observed when the air volume of SCC was 250 ml. Therefore, a pulsatility similar to that in the living human body was qualitatively achieved in the present circulation circuit. However, negative pressure was shown at the LVP, and reductions in the

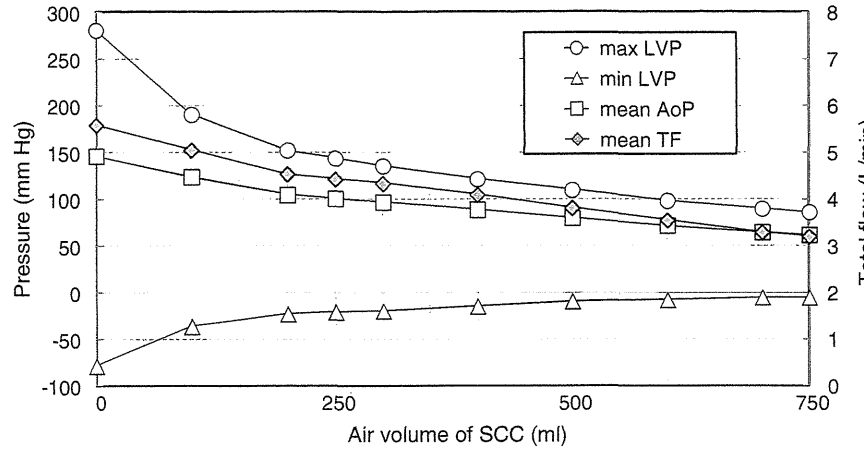

Fig. 4 SCC characteristics

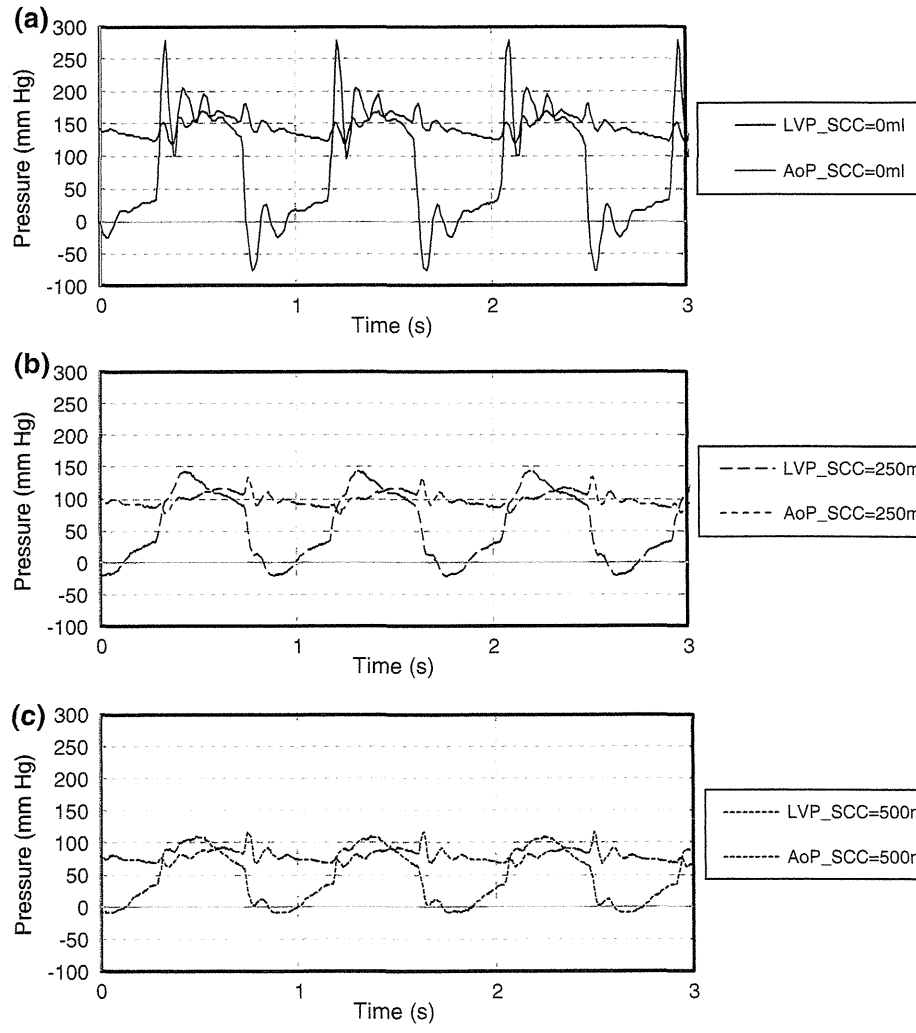

Fig. 5 LVP and AoP waveform when air volume of SCC is 0, 250 and 500 ml. **a** SCC = 0 ml. **b** SCC = 250 ml. **c** SCC = 500 ml

maximum value and phase lag in AoP against the LVP were shown, as compared with pressure wave forms in the living human body.

Evaluation of the range of reproducible circulatory conditions

Figure 6 shows the fundamental performance when the fluid resistance was changed from 100 % to 20–60 % in each given HR at SCC air volume of 250 ml. The max and min LVP and mean AoP were plotted against the TF for every HR and are shown in Fig. 6a, b, respectively. In each HR, the highest TF was observed in the gate opening of 100 %. When the gate opening was reduced, the decrease in the TF and increase in each pressure were observed. The same characteristic was found in every HR. The maximum range for each pressure and TF was near 300 mmHg and 10 l/min, respectively.

Figure 7 shows the fundamental performance when the air volume of SCC was 0, 250 and 500 ml. As an example, the performance at HR of 70 bpm is shown. When the air volume of SCC increased to 250 or 500 ml, the pressure and TF ranges decreased. The slope was nearly perpendicular to TF when the air volume of SCC was 0 ml.In contrast, the slope decreased gradually with increasing air volume of SCC. The same tendency was shown in other HR.

Figure 8 shows the fundamental performance when SL of the pulsatile pump was 50, 75 and 100 %. As an example, the performance at HR of 120 bpm is shown. In terms of decreasing the SL, the range of pressure and TF decreased with SL, as well as with decreasing air volume of SCC. However, the slope was maintained and a shift to the low TF region was shown. The same tendency was shown in other HR.

Long-term continuous operation experiment

Figure 9 shows the result for the long-term continuous operation experiment. Each plot shows the mean values for LVP, AoP, LAP, TF and temperature of working fluid, averaged for 1 h each day under steady circulatory conditions. Although pressure and TF decreased with human errors (failure of air valve closing in closed chamber) after 90 days, average values were almost constant over the six-month experiment. Continuous operation of the endurance test system was possible for 6 months without leakage or industrial device failure.

In terms of the diaphragm of the pulsatile pump, fatigue, fractures and leakage along its circumference were not observed. In addition, each sensor used in the rated range was also able to measure the data for 6 months without failure. However, it was necessary to adjust the air volume of SCC and closed chamber in order to maintain the initial condition twice a week over the experimental period, and replenishment of tap water due to evaporation was also necessary.

Figure 10 shows the LVP and AoP pressure wave forms on the first day and after 6 months. Although pulsatility did not change, spikes and oscillating components increased for each wave form.

Discussion

Effect of SCC and reproduction of pulsatility of pressure wave forms

The pressure wave forms generated in the present endurance test system had a pulsatility similar to that in the living human body because the range of pressures was

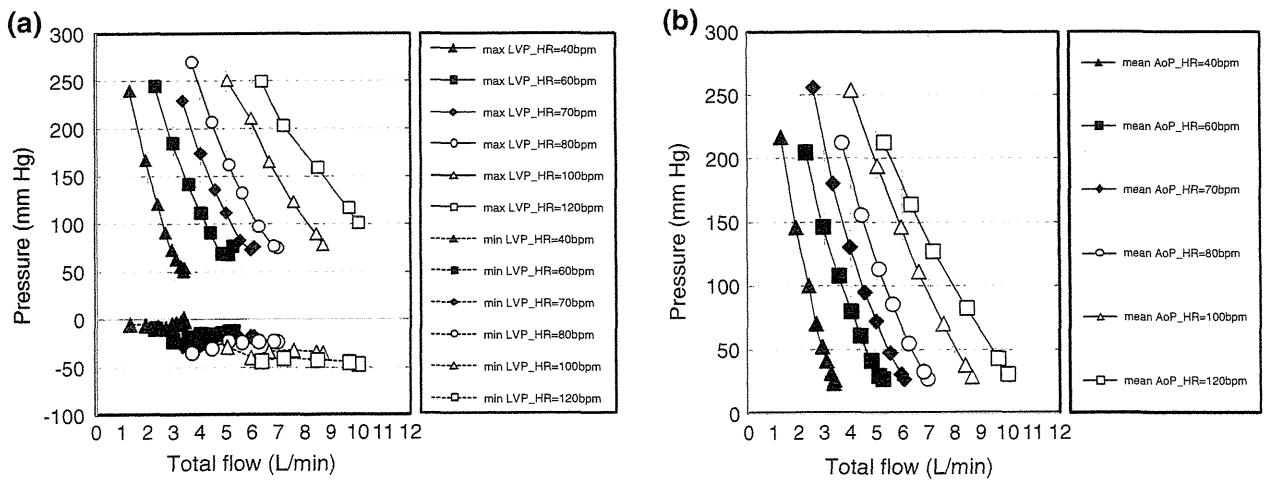

Fig. 6 Pressure-TF characteristics (SCC = 250 ml, SL = 100 %). **a** Max LVP, min LVP-TF characteristics. **b** Mean AoP-TF characteristics

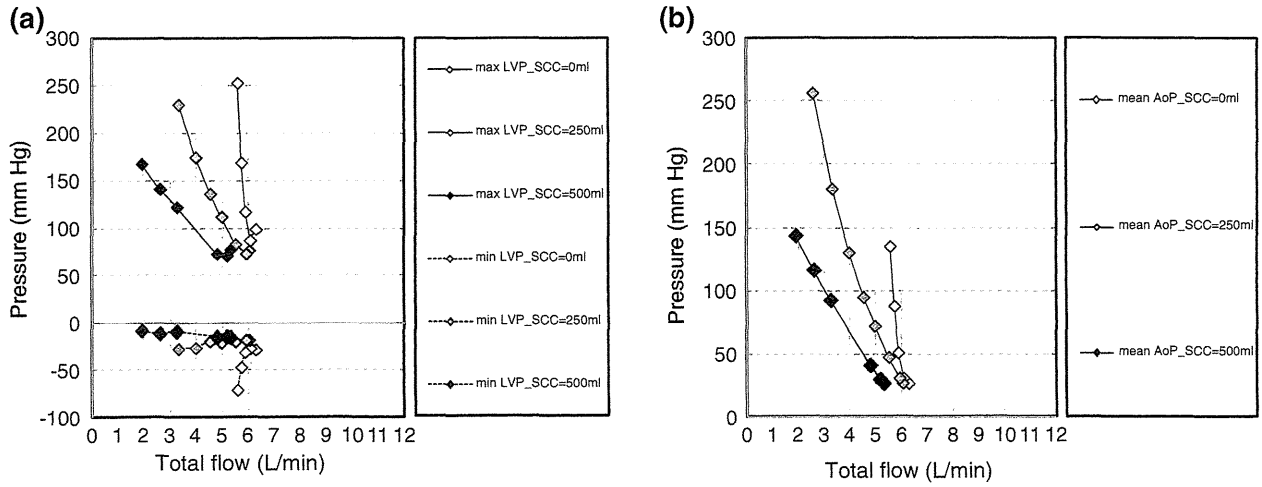

Fig. 7 Pressure-TF characteristics (SCC = 0, 250, 500 ml, SL = 100 %, HR = 70 bpm). **a** Max LVP, min LVP-TF characteristics. **b** Mean AoP-TF characteristics

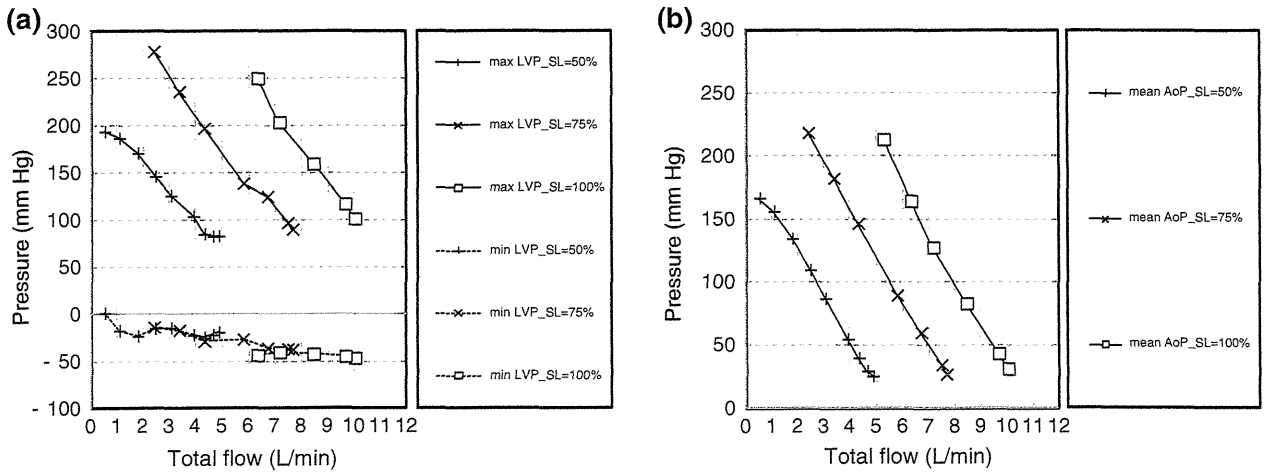

Fig. 8 Pressure-TF characteristics (SCC = 250 ml, SL = 50, 75, 100 %, HR = 120 bpm). **a** Max LVP, min LVP-TF characteristics. **b** Mean AoP-TF characteristics

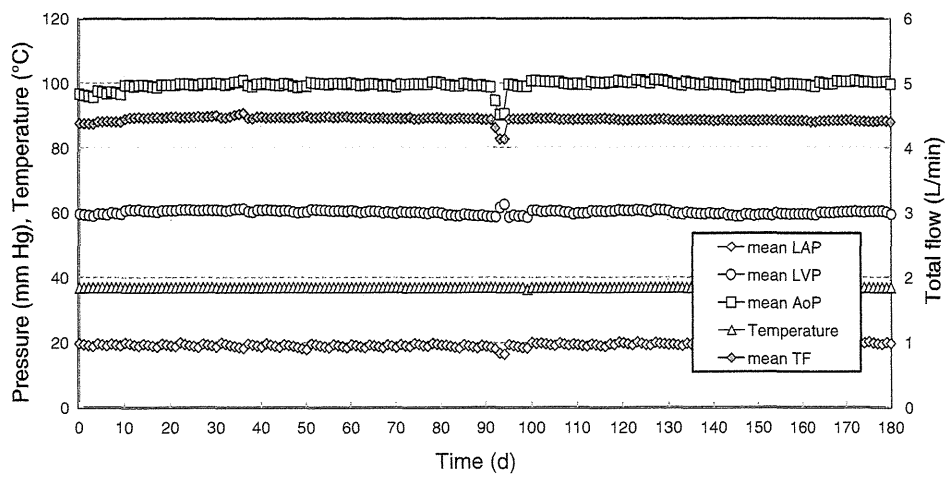

Fig. 9 Long-term continuous operation experiment for 6 months

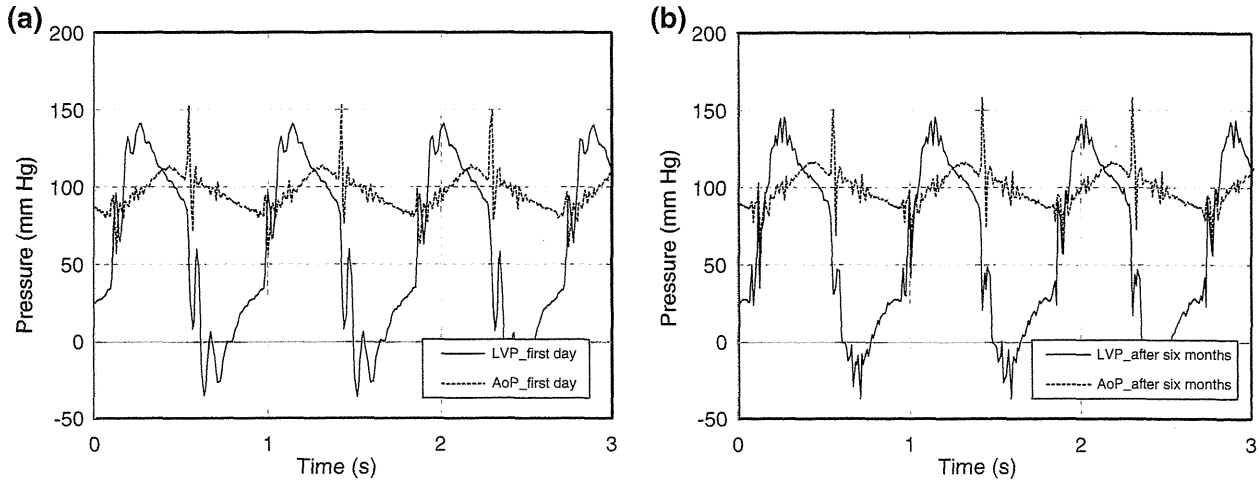

Fig. 10 LVP and AoP waveform on first day and after 6 months in long-term continuous operation experiment. **a** First day. **b** After 6 months

comparable compared with defined pressure values in Table 2. Examination of VADs under pulsatile conditions using this endurance test system is possible. In general, it is thought that the negative pressure of LVP does not occur in normal hemodynamics in the living human body. However, a negative pressure of LVP in the diastolic phase was shown. And this negative pressure was causally related to the pulsatile pump, which had an active filling mechanism. Because the pulsatile pump had more than 10 years operational experience in the industry, this active filling mechanism was adopted in order to give better durability. Hence, the negative pressure could be eliminated using a passive filling mechanism, similar to the native heart. A phase difference was observed between LVP and AoP wave forms. This was attributed to the resistance of the pipe which was attached between the outlet valve and the closed chamber and the compliance of the closed chamber. If the phase difference is large, the pressure load condition (pressure difference) to VAD changes even if the values of LVP and AoP are equivalent to the living human body. Therefore, an investigation of the relationship between pipe resistance and the compliance of the closed chamber will be necessary in order to make the phase difference as small as possible.

As a result of the relationship between the output of the pulsatile pump and the air volume of SCC, the pulsatile pump output could be quantitatively adjusted by changing the compliance of the pulsatile pump. Here, the increase in the compliance equals the decrease in the contractility because the compliance is the reciprocal of the elastance. Thus, a change in the contractility of the pulsatile pump forms against the pressure wave occurs as a result of the pressure wave varying the compliance of the pulsatile pump. Here, the dP/dt was calculated from each one cardiac cycle at LVP wave form that was measured for 1 min and expressed as a mean value with its standard deviation. The dP/dt at SCC air volumes of 0, 250 and 500 ml were 7313.0 ± 140.3, 1786.3 ± 48.2 and 1778.0 ± 40.0 mmHg/s, respectively. It is reported that the dP/dt in normal are approximately 1600 mmHg/s [23]. The dP/dt comparable to a living human body was shown when the air volume of SCC was 250 and 500 ml. However, a comparison of the dp/dt in each air volume of SCC showed that, although the dP/dt was decreased when the air volume of SCC was increased from 0 to 250 ml, changes in the dP/dt were not seen when the air volume of SCC was 250 and 500 ml. This may be due to the motion of the diaphragm in the shape of a sine wave in the pulsatile pump. In future studies, in order to reproduce further wide range circulation conditions like the reappearance of further low dP/dt, it is necessary to examine the motion of the diaphragm in the pulsatile pump or the SCC capacity; nonetheless, the present endurance test system showed pulsatility which can evaluate the VADs. Subsequently, the contractility of the pulsatile pump will be examined in order to obtain a pressure wave form more similar to that of hemodynamics in the living human body.

Evaluation of the range of reproducible circulatory conditions

In the measurement of fundamental performance, the circulation circuit was able to produce a wide range of pressure (maximum range, 300 mmHg) and TF (maximum range, 10 l/min) conditions. There is no compliance of the pulsatile pump when the air volume of SCC is 0 ml. Hence, even if the PR varied, the TF were not changed. TF were dependent on HR (Fig. 7). In addition, it is difficult to simulate the conditions containing compliance like the living human body because an excessive spike or negative

pressure occurred without compliance in Fig. 5 (air volume of SCC = 0 ml). The increase of air volume in the SCC allowed a decrease of pulsatile pump output, and the change in slope in the case of fundamental performance of SCC originated in the change in pulsatile pump compliance. Thus, the pulsatile pump became the condition containing the compliance (Fig. 7), and pressure wave forms could be generated without the excessive spike in Fig. 5 (air volume of SCC = 250, 500 ml). It was thought that our endurance test system which used industrial devices allowed the simulation of circulatory conditions by using the SCC, as well as the test equipment which used a flexible diaphragm or sack. In addition, although the range of pressure and TF became narrow when decreasing the proportion of SL, simulation of a low flow domain ($\leq$3 l/min) became possible (Fig. 8). As a result, defined pressure ranges within the children circulatory condition were observed when the SL was 50 %. Therefore, it is thought that this equipment will be applicable to endurance testing of VADs for children because the above circulatory conditions of children can be reproduced using this equipment. The endurance test system can be thought to generate not only adult but also children circulatory conditions by combining both SCC and SL function.

Long-term continuous operation experiment

The selected components of the endurance test system showed durability and stability for 6 months. However, when comparing the LVP and AoP data from the first day and after 6 months, some augmentation of spikes and oscillations was observed. This was thought to be caused by the valves mounted in the pulsatile pump; fatigue of the duckbill valves probably resulted from the pressure load of the pulsatile pump when opening and closing the valves. Progression of valve fatigue would affect the valve opening and closing performance, resulting in an insufficient closure and an increase in back-flow. Although there was no influence of the valves on mean TF for 6 months, back-flow might probably increase in long-term evaluation periods beyond 6 months. Therefore, it may be necessary to improve the valve design and materials in order to improve durability for further long-term evaluation.

The diaphragm of the pulsatile pump was made of rubber, as well as the valve, it was 1 cm in thickness, and although the rigidity was high, its compliance was low. The compliance of the pulsatile pump could be adjusted without affecting durability by connecting the SCC to the pulsatile pump. If the diaphragm was thin, it could fracture due to fatigue. Therefore, the use of the SCC was thought to be effective for maintaining diaphragm durability. In terms of the reservoir which is open to the atmosphere, water refilling was necessary due to evaporation, and this was disadvantageous for a long-term continuous operation experiment. Therefore, it may be necessary to attempt a closed chamber which approximates the LA in our endurance test system. Although it is necessary to improve the valves and the reservoir, the present endurance test system showed durability and stability and allowed 6 months evaluation. This time the 6 months continuous experiment was performed supposing the minimum period of the endurance test in the guideline [21]. Hence, more than 6 months continuous operation experiment was not carried out. In addition, a practical examination of VADs was not performed. In future studies, evaluation of more than 6 months continuous operation and durability testing of VADs will be necessary in order to validate the usefulness of the present endurance test system.

Conclusions

We developed a novel endurance test system and evaluated its basic performance and long-term durability and stability. The developed endurance test system showed a wide range of reproducible circulatory conditions, durability and stability through the use of an SCC and industrial devices. This endurance test system is potentially useful for evaluating the basic characteristics of VADs.

Acknowledgments The present study was supported by Grants-in-Aid for Scientific Research A (no. 23249065 and no. 21249076) and B (no. 21390398) from the Ministry of Education, Culture, Sports, Science and Technology of Japan, and by the Intramural Research Fund (22-3-3) for Cardiovascular Diseases from the National Cerebral and Cardiovascular Center.

References

1. Frazier OH, Myers TJ, Gregoric ID, Khan T, Delgado R, Croitoru M, Miller K, Jarvik R, Westaby S. Initial clinical experience with the Jarvik 2000 implantable axial-flow left ventricular assist system. Circulation. 2002;105:2855–60.
2. Wieselthaler GM, Schima H, Hiesmayr M, Pacher R, Laufer G, Noon GP, DeBakey M, Wolner E. First clinical experience with the DeBakey VAD continuous-axial-flow pump for bridge to transplantation. Circulation. 2000;101:356–9.
3. Frazier OH, Delgado RM 3rd, Kar B, Patel V, Gregoric ID, Myers TJ. First clinical use of the redesigned HeartMate II left ventricular assist system in the United States: a case report. Tex Heart Inst J. 2004;31:157–9.
4. Griffith K, Jenkins E, Pagani FD. First American experience with the Terumo DuraHeart left ventricular assist system. Perfusion. 2009;24:83–9.
5. Marlinski E, Jacobs G, Deirmengian C, Jarvik R. Durability testing of components for the Jarvik 2000 completely implantable axial flow left ventricular assist device. ASAIO J. 1998; 44(5): M741–4.
6. Anderson DW. Blood pumps: technologies and markets in transformation. Artif Organs. 2001;25:406–10.

7. Mizuguchi K, Damm GA, Bozeman RJ, Akkerman JW, Aber GS, Svejkovsky PA, Bacak JW, Orime Y, Takatani S, Nosé Y, Noon GP, DeBakey ME. Development of the Baylor/NASA axial flow ventricular assist device: in vitro performance and systematic hemolysis test results. Artif Organs. 1994;18:32–43.
8. Nojiri C, Kijima T, Maekawa J, Horiuchi K, Kido T, Sugiyama T, Mori T, Sugiura N, Asada T, Umemura W, Ozaki T, Suzuki M, Akamatsu T, Westaby S, Katsumata T, Saito S. Development status of Terumo implantable left ventricular assist system. Artif Organs. 2001;25:411–3.
9. Yamane T, Maruyama O, Nishida M, Kosaka R, Sugiyama D, Miyamoto Y, Kawamura H, Kato T, Sano T, Okubo T, Sankai Y, Shigeta O, Tsutsui T. Hemocompatibility of a hydrodynamic levitation centrifugal blood pump. J Artif Organs. 2007;10(2): 71–6. Epub 2007 Jun 20.
10. Umezu M, Yamazaki K, Yamazaki S, Iwasaki K, Miyakoshi T, Kitano T, Tokuno T. Japanese-made Implantable Centrifugal Type Ventricular Assist System (LVAS): EVAHEART. Biocybern Biomed Eng. 2007;27:111–9.
11. National Institute of Advanced Industrial Science and Technology. R&D Working Group report for active implants: innovative artificial heart systems. 2006. http://www.aist.go.jp/aist_j/aistinfo/report/entrust/iryoukiki/2006/techrep_artificalheart_ft2006.pdf. Accessed 25 April 2012 (in Japanese).
12. Yokoyama Y, Kawaguchi O, Shinshi T, Steinseifer U, Takatani S. A new pulse duplicator with a passive fill ventricle for analysis of cardiac dynamics. J Artif Organs. 2010;13:189–96.
13. Pantalos GM, Koenig SC, Gillars KJ, Giridharan GA, Ewert DL. Characterization of an adult mock circulation for testing cardiac support devices. ASAIO J. 2004;50(1):37–46.
14. Gibber M, Wu ZJ, Chang WB, Bianchi G, Hu J, Garcia J, Jarvik R, Griffith BP. In vivo experience of the child-size pediatric Jarvik 2000 heart: update. ASAIO J. 2010;56(4):369–76.
15. Litwak P, Butler KC, Thomas DC, Taylor LP, Macha M, Yamazaki K, Konishi H, Kormos RL, Griffith BP, Borovetz HS. Development and initial testing of a pediatric centrifugal blood pump. Ann Thorac Surg. 1996;61:448–51.
16. Weiss WJ. Pulsatile pediatric ventricular assist devices. ASAIO J. 2005;51(5):540–5.
17. Kitao T, Ando Y, Yoshikawa M, Kobayashi M, Kimura T, Ohsawa H, Machida S, Yokoyama N, Sakota D, Konno T, Ishihara K, Takatani S. In vivo evaluation of the "TinyPump" as a pediatric left ventricular assist device. Artif Organs. 2011;35: 543–53.
18. Timms D, Hayne M, McNeil K, Galbraith A. A complete mock circulation loop for the evaluation of left, right, and biventricular assist devices. Artif Organs. 2005;29:564–72.
19. Fleming S, Thompson M, Stevens R, Heneghan C, Plüddemann A, Maconochie I, Tarassenko L, Mant D. Normal ranges of heart rate and respiratory rate in children from birth to 18 years of age: a systematic review of observational studies. Lancet. 2011;377: 1011–8.
20. Park MK, Menard SW, Schoolfield J. Oscillometric blood pressure standards for children. Pediatr Cardiol. 2005;26(5):601–7.
21. Ministry of Economy, Trade and Industry. R&D Guidelines for active implants 2007: innovative artificial heart systems. 2007. http://www.meti.go.jp/policy/mono_info_service/service/iryou_fukushi/downloadfiles/200705-2.pdf. Accessed 25 April 2012 (in Japanese).
22. Kiani A, Gilani Shakibi J. Normal value of left ventricular end-systolic elastance in infants and children. IJMS. 2003;28:169–72.
23. Smith JJ, Kampine JP. Circulatory physiology: the essentials. Lippincott Williams and Wilkins, Baltimore; 1984.

P#19

Preclinical Evaluation of a Cardiopulmonary Support System Consisting of the Newly-Developed Centrifugal Pump with a Unique Hydrodynamic Bearing

Presenter: Tomonori Tsukiya

Institute: National Cerebral & Cardiovascular Center

Subject: Rotary blood pumps in extracorporeal circulation / pediatric and adult circulation

Author 1: Toshihide Mizuno, National Cerebral & Cardiovascular Center

Author 2: Yoshiaki Takewa, National Cerebral & Cardiovascular Center

Author 3: Takashi Yamane, National Institute of Advanced Indutrial Science and Technology

Author 4: Hideo Hoshi, Mitsubishi Heavy Industries, Ltd.

Author 5: Takeshi Okubo, Mitsubishi Heavy Industries, Ltd.

Author 6: Toshiyuki Osada, Mitsubishi Heavy Industries, Ltd.

Author 7: Eisuke Tatsumi, National Cerebral & Cardiovascular Center

Author 8: Yoshiyuki Taenaka, National Cerebral & Cardiovascular Center

Purpose: The purpose of the study is to evaluate durability, in vivo hemodynamics, and biocompatibility of a newly developed durable cardiopulmonary support system consisting of a compact centrifugal blood pump with the unique hydrodynamically levitated impeller.

Methods: The centrifugal pump including the driving motor has the 123 mm of length and 59 mm of diameter, weighing 500 grams. The disposable pump head made of polycarbonate employs a unique hydrodynamic bearing in which the impeller is suspended by two independent journal bearings. In vivo study was conducted by making a veno-arterial bypass between the inferior vena cava and the carotid artery with the newly developed centrifugal pump and the membrane oxygenator with anticoagulant coating into four Japanese Saanen goats weighing from 50 to 60 kg. After installation, the devices were fixed to the specially designed harness, and the animals were kept in the cage for the scheduled 30 postoperative days. No anticoagulant therapy was employed except for during the surgical procedure.

Results: Three goats survived for 30 days and were electively terminated. One goat died of bleeding at 21 POD due to the rupture of the carotid artery. The cardiopulmonary support systems were able to deliver stably 2.79[plusmn]0.29 L/min of blood flow. The plasma free hemoglobin level increased during the first week up to 12.5 mg/dL, but returned and stayed within the normal range. The blood contacting surfaces of the explanted centrifugal pumps were free of thrombus for all cases. Small amount of thrombus was observed on the casing of the membrane oxygenator after 30 days in all cases, but the gas transfer was kept within normal.

Conclusions: In conclusion, the newly developed hydrodynamically levitated centrifugal blood pump and the membrane oxygenator demonstrated sufficient durability and excellent biocompatibility as a long-term cardiopulmonary support system.

Artificial Organs

Abstract: Coronary circulation is closely linked to myocardial oxygen consumption (MVO_2), and previous reports have suggested decreased coronary flow (CoF) under left ventricular assist device support. Decreased CoF itself under support is not unfavorable because the native heart can be well unloaded and myocardial oxygen demand is also decreased. There should be an autoregulatory system that would maintain optimal CoF according to oxygen demand; however, the detailed mechanism is still unclear. The aim of the current study is to evaluate the effect of centrifugal pumps on CoF under varied bypass rates in relation to left ventricle workload. A centrifugal pump, EVAHEART (Sun Medical Technology Research Corporation, Nagano, Japan), was installed in an adult goat ($n = 10$, 61.3 ± 6.5 kg). We set up the following conditions, including Circuit-Clamp (i.e., no pump support), 50% bypass, and 100% bypass. In these settings, CoF, MVO_2, pressure–volume area (PVA), and coronary vascular resistance (CVR) were measured. In 100% bypass, CoF, MVO_2, and PVA were all decreased significantly from clamp. While in 50% bypass, CoF and MVO_2 decreased from clamp, but not PVA. There was a significant 40% increase in CVR in 100% bypass from clamp. This CVR increase in 100% bypass was possibly due to mechanical collapse of coronary vascular bed itself by pump support or increased vascular tone through autoregulatory system. In clinical settings, we should adjust optimal pump speed so as not to cause this vascular collapse. However, to clarify autoregulatory system of the coronary perfusion, further investigation is ongoing in ischemic and heart failure models. **Key Words:** Left ventricular assist device—Myocardial perfusion—Myocardial oxygen demand.

Coronary Vascular Resistance Increases Under Full Bypass Support of Centrifugal Pumps—Relation Between Myocardial Perfusion and Ventricular Workload During Pump Support

*†Masahiko Ando, *Yoshiaki Takewa, †Takashi Nishimura, ‡Kenji Yamazaki, †Shunei Kyo, §Minoru Ono, *Tomonori Tsukiya, *Toshihide Mizuno, *Yoshiyuki Taenaka, and *Eisuke Tatsumi

*Department of Artificial Organs, National Cerebral and Cardiovascular Center Research Institute, Osaka; †Department of Therapeutic Strategy for Heart Failure; §Department of Cardiothoracic Surgery; University of Tokyo; and ‡Department of Cardiovascular Surgery, Tokyo Women's Medical University, Tokyo, Japan

doi:10.1111/j.1525-1594.2011.01298.x

Received September 2010; revised February 2011.

Address correspondence and reprint requests to Dr. Masahiko Ando, Department of Artificial Organs, National Cerebral and Cardiovascular Center Research Institute, 5-7-1 Fujishiro-dai, Suita, Osaka 565-8565, Japan. E-mail: masandoo@hotmail.com

Presented in part at the 2010 ESAO Meeting held September 8–12, 2010 in Skopje, Macedonia.

Coronary circulation is closely linked to myocardial oxygen consumption (MVO_2) (1,2), and previous reports have suggested decreased myocardial perfusion under left ventricular assist device (LVAD) support (3–5). Decreased coronary blood flow during LVAD support in itself is not unfavorable because the native heart can be well unloaded with support and myocardial oxygen demand is also decreased (6,7). There should be an autoregulatory system of coronary blood flow that would maintain optimal myocardial perfusion according to its oxygen demand (1,2,8), and the system could eliminate excessive coronary blood flow when the workload of the native heart is decreased. This intricate regulation has been thought for many years to be through sympathetic neuronal control (9) or chemical mediators, such as adenosine, ATP-dependent K+ channels, nitric oxide, prostaglandins, or inhibition of endothelin (10,11); however, its mechanism in detail has been unclear even to date. (2) Theoretically, the chief and direct determinants of coronary blood flow are: heart rate, arterial blood pressure, especially diastole, and coronary vascular resistance (CVR) (1,12). Out of these three factors, CVR is of great importance especially under LVAD support because it can be affected

by coronary vascular tone, intraventricular pressure, and ventricular wall tension (8). Therefore, we have come to survey the changes in coronary perfusion and CVR under LVAD support.

In the present study, we mainly focused on the effect of a centrifugal LVAD on the amount of coronary flow (CoF) in a normal heart model, in both half and full bypass condition. The influence of LVAD support on myocardial perfusion can be of course different among pump types (13,14), bypass rates (4,6,15), and the native heart function (5,16). In order to build up basic theory, we first did the study in a normal heart model. In previous studies in pulsatile pumps, CoF is normally decreased by support in normal heart model (4) and increased in heart failure model (5,14); however, studies in rotary pumps are still limited and the results are different among reports. The one major difference between pump types is that in pulsatile pumps, the native heart can dilate more easily when pumps are ejecting, while in rotary pumps, the native heart relaxation is more difficult because pumps are continuously ejecting through systole and diastole. Another major difference between axial and centrifugal pump is the flow difference in one cardiac cycle. It can vary more in centrifugal LVAD support due to its mechanical feature (17). In other words, in centrifugal pumps, diastolic flow can be decreased when the pressure head (i.e., aortic pressure [AoP]–left ventricular pressure) becomes relatively high, and this feature might affect coronary perfusion. Indeed, Voitl et al. had reported that coronary perfusion did not decrease by axial pump support in a normal heart model (18).

The aim of the current study is to evaluate the effect of centrifugal pumps on coronary circulation under varied bypass rate in relation to left ventricle (LV) workload. Especially, we focused on the changes in CVR and made some medical and physiological suggestions under rotary LVAD support in clinical practice.

MATERIALS AND METHODS

Experiments were performed on 10 adult goats (61.3 ± 6.5 kg). The animals were fixed in the right recumbent position and intubated. Via left thoracotomy, pressure lines for AoP and central venous pressure (CVP) monitoring were established. We placed an 18 mm electromagnetic flow probe (EMF-1000, Nihon Kohden, Tokyo, Japan) for monitoring ascending aortic flow (AoF). An ultrasonic flow probe (HQD3FSB, Transonic System, Inc., Ithaca, NY, USA) was attached for the monitoring of CoF on the main trunk of the left coronary artery. A 16-mm outflow cannula was sutured to the descending aorta, and 16 mm ultrasonic flow probe (TS420, Transonic) was placed for the monitoring pump flow (PF). After systemic heparinization, a 20-mm inflow cannula was inserted into the LV from the apex. Both the outflow and inflow cannulae were connected to the EVA-HEART (Sun Medical Technology Research Corporation, Nagano, Japan) (17), and we started left heart bypass. A 4Fr Mikro-tip catheter pressure transducer (Millar Instruments, Houston, TX, USA) and a 6Fr conductance catheter (2S-RH-6DA-116, 6 mm, Taisho Biomed Instrument Co., Ltd, Osaka, Japan) were inserted from the anterior wall of the LV for the monitoring of pressure–volume loop (PV loop). The inferior vena cava was taped for the preload reduction to obtain end-systolic pressure–volume relationship (ESPVR). All these experimental protocols were approved by the Animal Research Committee of the National Cerebral and Cardiovascular Center Research Institute and conducted according to its guidelines under the care of a veterinarian.

In the present study, we set up the following three conditions: (A) Circuit-Clamp (i.e., no pump support); (B) 50% bypass; and (C) 100% bypass. Bypass rate was calculated by dividing PF by the sum of PF and AoF. Systemic vascular resistance (SVR) was calculated by dividing the difference between AoP and CVP by total flow, which is the sum of PF and AoF. CVR was calculated by dividing that difference by CoF. SVR and CVR were shown in the ratio, regarded the value in (A) clamp as a baseline. After the experiment, we measured the weight of the LV, and CoF was normalized to the amounts per the LV 200 g.

A 10-Fr retrograde cardioplegic catheter (Gandry RCSP catheter, 94110, Medtronic Japan Co., Ltd, Tokyo, Japan) was inserted to the coronary sinus through the left azygos vein. A balloon was inflated and coronary vein blood was drawn from the small hole which was manually made just before the balloon. We calculated MVO_2 using the following formula as previously reported (4,6,7,18).

$$MVO_2(O_2\ mL/min) = \{(ScaO_2 - ScvO_2) \times 1.34 \times aHb + (PcaO_2 - PcvO_2) \times 0.003\} \times 0.01 \times CoF\ (mL/min)$$

where $ScaO_2$ ($ScvO_2$) = oxygen saturation of the coronary artery (vein) blood; $PcaO_2$ ($PcvO_2$), mm Hg = partial pressure of the coronary artery (vein) blood; and aHb, g/dL = hemoglobin concentration of the coronary artery blood. In the results, we showed normalized MVO_2 per beat per LV weight of 100 g. We also showed $SatO_2$ gap (i.e.,

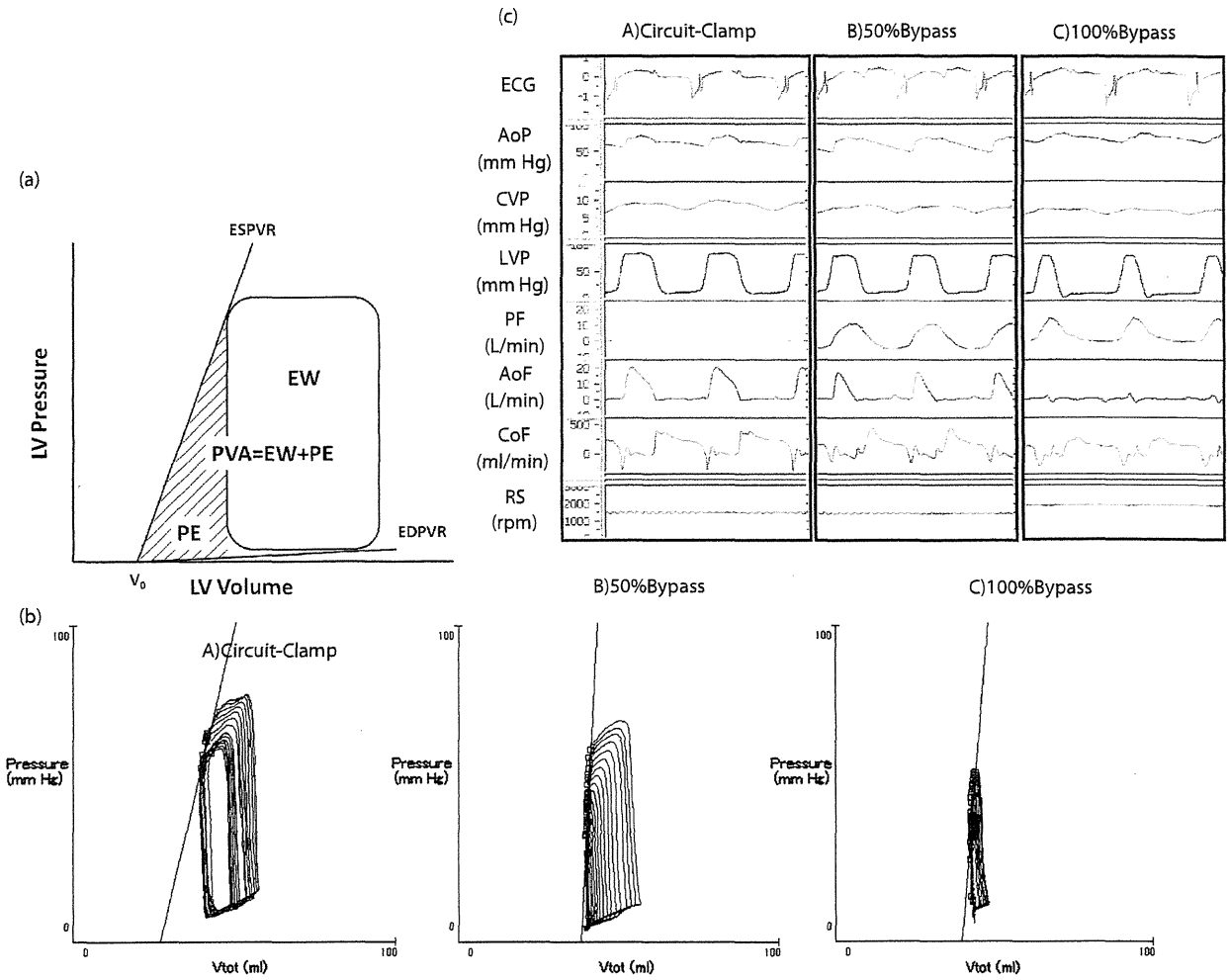

FIG. 1. (a) Schema of pressure–volume loop. PVA is a sum of EW and PE. EW, external work; PE, potential energy; PVA, pressure–volume area; ESPVR, end-systolic pressure–volume relationship; EDPVR, end-diastolic pressure–volume relationship; V_0, *X*-axis intercept of the ESPVR slope. (b) Pressure and flow waveforms. ECG, electrocardiogram; AoP, aortic pressure; CVP, central venous pressure; LVP, left ventricular pressure; PF, pump flow; AoF, ascending aortic flow; CoF, coronary flow; RS, rotational speed. (c) Pressure–volume loops in varied bypass rates. Similar loops were obtained in both (A) and (B) conditions. In (C) conditions, loop size is much smaller than the other two conditions.

$=ScaO_2 - ScvO_2$), which is a main determinant of MVO_2 as well as CoF.

Sigma5 DF system (CD Leycom, Zoetermeer, The Netherlands) was used for the PV loop analysis. The slope of the ESPVR was obtained by gradually occluding the inferior vena cava (7). Pressure–volume area (PVA), which has been recognized as a measure of total mechanical energy and correlates linearly with MVO_2 regardless of changes in loading conditions (19), was approximated by the previously established method (7,19). Briefly, as shown in Fig. 1a, external work (EW) is a computed area in the PV loop, and potential energy (PE) is a crescent area between the ESPVR slope and the straight line of isovolumic relaxation (Fig. 1a). PVA is a sum of EW and PE and is shown in the normalized value per left ventricular weight of 100 g.

The comparison was performed by repeated analysis of variance followed by Tukey's multiple comparison test, and *P* value less than 0.05 was considered as statistically significant.

RESULTS

Figure 1b shows sample waveforms of pressure and flow data. In (B) 50% bypass, when PF and AoF become nearly equal, a small amount of negative PF can be seen in the late diastole, and diastolic AoP

TABLE 1. *Changes in hemodynamic parameters by varied assist rates*

Mode	(A) Clamp	(B) 50% bypass	(C) 100% bypass
Heart rate (rpm)	85.4 ± 8.8	82.1 ± 12.5	80.4 ± 14.4
Mean CVP (mm Hg)	9.8 ± 2.5	9.9 ± 2.4	9.9 ± 2.6
Mean AoP (mm Hg)	66.5 ± 10.7	64.2 ± 9.7	68.2 ± 10.7
Diastolic AoP (mm Hg)	60.5 ± 10.8	58.7 ± 10.0	66.1 ± 10.8
Mean LVP (mm Hg)	46.0 ± 6.5	41.9 ± 8.3	31.1 ± 9.1*†
RS (rpm)	0.0 ± 0.0	1520 ± 162*	2100 ± 149*†
PF (L/min)	0.00 ± 0.00	2.03 ± 0.64*	3.93 ± 1.51*†
AoF (L/min)	4.51 ± 1.30	1.94 ± 0.59*	0.28 ± 0.47*†
Bypass rate (%)	0.0 ± 0.0	51.0 ± 0.6*	93.5 ± 11.1*†
ESP (mm Hg)	81.7 ± 7.9	81.8 ± 14.0	68.7 ± 16.2*†
EDP (mm Hg)	16.0 ± 3.2	15.3 ± 3.3	13.0 ± 3.6*†
ESV (mL)	53.4 ± 10.9	54.3 ± 11.4	53.9 ± 11.7
EDV (mL)	75.3 ± 15.3	75.0 ± 16.4	67.4 ± 15.2*†
Mean CoF (mL/min/LV 200 g)	135.9 ± 29.3	116.7 ± 19.5*	113.5 ± 27.3*
$SatO_2$ gap	0.51 ± 0.10	0.53 ± 0.10	0.41 ± 0.13*†
Hb (g/dL)	9.8 ± 1.7	9.7 ± 1.9	9.6 ± 1.7
MVO_2 (mL/beat/LV 100 g)	0.057 ± 0.012	0.051 ± 0.010*	0.039 ± 0.012*†
PVA (mL × mm Hg/LV100 g)	1246.9 ± 322.3	1276.4 ± 402.0	707.8 ± 380.0*†
EW (mL × mm Hg/LV 100 g)	829.4 ± 248.8	819.4 ± 268.7	402.8 ± 183.9*†
PE (mL × mm Hg/LV 100 g)	417.5 ± 143.2	457.0 ± 254.8	305.6 ± 221.0*†
SVR ratio	1.00 ± 0.0	1.05 ± 0.31	1.15 ± 0.44
CVR ratio	1.00 ± 0.0	1.20 ± 0.37	1.35 ± 0.47*

* means significant change from (A); † means significant change from (B) condition.

CVP, central venous pressure; AoP, aortic pressure; LVP, left ventricular pressure; RS, rotation speed; PF, pump flow; AoF, ascending aortic flow; ESP, end-systolic pressure; EDP, end-diastolic pressure; ESV, end-systolic volume; EDV, end-diastolic volume; CoF, coronary flow; Sat O_2 gap, saturation difference between coronary artery and vein blood; Hb, hemoglobin concentration; MVO_2, myocardial oxygen consumption; PVA, pressure–volume area; EW, external work; PE, potential energy; SVR ratio, systemic vascular resistance ratio regarded (A) as a baseline; CVR ratio, coronary vascular resistance ratio regarded A) as a baseline.

seems to be reduced compared with the other two conditions. In (C) 100% bypass, almost no AoF was observed, and the retrograde flow in diastolic phase was not found at all. As for the waveform of CoF in (A) and (B) conditions, there were flow peaks in the early diastole, while the peak disappeared in (C) 100% bypass, despite the fact that PF in the diastolic phase was well maintained (Fig. 1b).

Table 1 shows all numerical data. There was no significant change in heart rate, mean CVP, mean AoP, or diastolic AoP. In (C) 100% bypass, mean LVP was lower than the other two conditions.

In Fig. 1c, we have shown sample PV loops. In (B) 50% bypass, the loop was similar to that in (A) Clamp, while in (C) 100% bypass, it has become prominently smaller from those in both (A) Clamp and (B) 50% bypass. As shown in Table 1, PVA, EW, and PE were all decreased in (C) 100% bypass, and according to these changes, MVO_2 was also decreased in that condition (Table 1). We have also calculated LV pressure and volume, which revealed that end-systolic pressure, end-diastolic pressure, and end-diastolic volume were significantly decreased in (C) 100% bypass.

CoF was decreased in both (B) 50% and (C) 100% bypass (Table 1), but no difference was observed between these two conditions. In (C) 100% bypass, CVR ratio was significantly increased (Table 1).

DISCUSSION

In the current study, we have investigated left ventricular mechanics and myocardial perfusion during centrifugal LVAD support at varied bypass rates, in relation to the left ventricular workload and MVO_2. In summary, in 50% bypass, LV workload was similar to that in clamp condition; however, CoF was decreased without any change in CVR ratio (Table 1). While in 100% bypass, LV workload was significantly decreased from both clamp and 50% bypass conditions, and CoF was decreased with significant increase in CVR ratio (Table 1).

In fact, few data are available to show the effect of centrifugal LVADs on myocardial perfusion. In the present study, we have measured not only CoF but also MVO_2 and PVA to clarify in detail the relation between these parameters. Our investigation here has made it evident that centrifugal LVADs can reduce CoF in normal heart in both half and full bypass conditions; however, the mechanism of reduced CoF can be different between these two conditions.

In (C) 100% bypass, the PV loop became prominently smaller than that in baseline (Fig. 1c), and PVA and MVO_2 were significantly decreased from both (A) and (B) conditions (Table 1). CoF was also decreased from baseline. As shown previously, MVO_2 is calculated by multiplying $SatO_2$ gap both by Hb and CoF. In the present study, there was no Hb deviation (Table 1); therefore, MVO_2 reduction is mainly due to reduction in CoF and $SatO_2$ gap. During the experiments, $ScaO_2$ was kept at almost 1.0 without exception. So, $SatO_2$ gap reduction actually indicates an increase in $ScvO_2$, which means the LV was effectively decompressed by the full bypass condition, and oxygen demand, or oxygen uptake from the coronary artery blood, was practically decreased.

These changes in the major determinants of MVO_2 during rotary LVAD support are yet to be clearly established even in the current era. Tuzun et al. has reported the decreased MVO_2 and CoF in the normal heart during axial flow LVAD support (4). There were no changes in MVO_2/CoF ratio by varied rotation speed, which indicates that no O_2 gap reduction was present by increasing rotation speed, assuming that there was no Hb deviation. Voitl et al. has suggested that CoF was not decreased by maximal axial pump support; however, MVO_2 was significantly decreased, which implies that MVO_2 reduction was mainly caused by $SatO_2$ gap reduction (18). Contrary to these reports, in the present study, both CoF and $SatO_2$ gap reduction has occurred in full bypass condition. In general, there should be a positive correlation between MVO_2 and CoF (1,2), and $SatO_2$ gap should be decreased under full support condition (1,8). Therefore, our results that both CoF and $SatO_2$ gap were decreased can be acceptable and compatible to the previous reports in physiology (1,2,19).

We have also focused on the changes in CVR, because the amount of CoF can be determined by the following three factors, that is to say, heart rate, AoP, especially diastolic, and CVR (1). In (C) 100% bypass, heart rate is lower than (A) Clamp (Table 1), but the difference was not significant. As for AoP, there was no mean or diastolic AoP deviation between groups. Thus, the key factor could be CVR, and CVR ratio was actually increased in (C) 100% bypass (Table 1). The reason why we obtained increased CVR in (C) 100% bypass is unknown, but we speculate that there should be an autoregulatory system of the coronary artery that might have eliminated the excessive oxygen supply under well-unloaded condition (2,8). There have been many researches on the chemical mediators related to regulation of myocardial perfusion; however, most of these studies focused on the vasodilative effect on the coronary vessels during exercise compared with resting condition (8,10,11,20–22), and the vasoconstrictive effect of these mediators during LVAD support compared with no support condition has yet to be investigated. More research is needed to clarify the autoregulatory mechanism of the coronary artery during LVAD support.

Another reason for the increased CVR in the full bypass condition could be due to the mechanical features of the rotary pump. In pulsatile pumps, there must be a pump systolic phase, and at least during this phase, the native heart can dilate because the mechanical valve between pump chamber and the native heart closes and no vacuum pressure can prevent the native heart from dilation. Whereas in the rotary pump, the situation is different. Rotary LVADs can continuously work through in one cardiac cycle, and especially in full bypass condition, it might affect dilation of the native heart. In diastolic dysfunction without coronary vessel disease, endocardial blood flow is known to be decreased possibly due to collapse of the coronary vascular bed (23). If rotary LVADs had prevented the native heart from dilation in the current study, in the worst case, it might have collapsed the coronary vascular bed, increased CVR, and decreased myocardial perfusion. In order to prevent these vascular bed collapses, we should adjust optimal pump rotational speed so as not to disturb myocardial dilation.

In (B) 50% bypass, a similar PV loop was obtained as in (A) Clamp (Fig. 1c). There were no obvious changes in PVA and pressure data (Table 1); however, a small amount of retrograde PF was observed (Fig. 1a). This retrograde flow was mainly seen in the diastolic phase, when the pressure head (i.e., AoP–LVP) becomes relatively high. Because of this reverse flow, we should definitely recognize that "Half Bypass" is quite different from "Half Support" in left heart bypass with rotary pumps, even if PF is half of the total flow. This reverse flow in half bypass condition was not always present and might have affected the results of the present study. The reason why we did not obtain significant decrease in PVA in (B) 50% bypass despite pump support was possibly due to this reverse flow, and the decrease in CoF in (B) 50% bypass might be caused by this retrograde PF (Table 1).

The present study was performed on normal hearts, and the study on ischemic hearts might have provided different results (5,14–16). Nevertheless, we believe that the current study is considered of value in that we have focused on CVR under rotary LVAD support.

CONCLUSION

CVR increases under full bypass support of centrifugal pumps. In clinical settings, we should adjust pump rotational speed at optimal settings so as not to cause coronary vascular bed collapse. As a physiological rationale, there should be an autoregulatory system of the coronary system, and further investigation is ongoing in ischemic and heart failure models.

REFERENCES

1. Feigl EO. Coronary physiology. *Physiol Rev* 1983;63:1–205.
2. Tune JD, Gorman MW, Feigl EO. Matching coronary blood flow to myocardial oxygen consumption. *J Appl Physiol* 2004;97:404–15.
3. Ootaki Y, Kamohara K, Akiyama M, et al. Phasic coronary blood flow pattern during a continuous flow left ventricular assist support. *Eur J Cardiothorac Surg* 2005;28:711–6.
4. Tuzun E, Eya K, Chee HK, et al. Myocardial hemodynamics, physiology, and perfusion with an axial flow left ventricular assist device in the calf. *ASAIO J* 2004;50:47–53.
5. Noda H, Takano H, Taenaka Y, et al. Regulation of coronary circulation during left ventricular assist. *ASAIO Trans* 1989;35:445–7.
6. Pennock JL, Pierce WS, Prophet GA, Waldhausen JA. Myocardial oxygen utilization during left heart bypass; effect of varying percentage of bypass flow rate. *Arch Surg* 1974; 109:635–41.
7. Kawaguchi O, Sapirstein JS, Daily WB, Pae WE, Pierce WS. Left ventricular mechanics during synchronous left atrial-aortic bypass. *J Thorac Cardiovasc Surg* 1994;107:1503–11.
8. Duncker DJ, Bache RJ. Regulation of coronary blood flow during exercise. *Physiol Rev* 2008;88:1009–86.
9. Haws CW, Green LS, Burgess MJ, Abildskov JA. Effects of cardiac sympathetic nerve stimulation on regional coronary blood flow. *Am J Physiol* 1987;252:H269–74.
10. Duncker DJ, van Zon NS, Ishibashi Y, Bache RJ. Role of k+ atp channels and adenosine in the regulation of coronary blood flow during exercise with normal and restricted coronary blood flow. *J Clin Invest* 1996;97:996–1009.
11. Farias M 3rd, Gorman MW, Savage MV, Feigl EO. Plasma atp during exercise: possible role in regulation of coronary blood flow. *Am J Physiol Heart Circ Physiol* 2005;288:H1586–1590.
12. Klocke FJ, Ellis AK, Orlick AE. Sympathetic influences on coronary perfusion and evolving concepts of driving pressure, resistance, and transmural flow regulation. *Anesthesiology* 1980;52:1–5.
13. Bartoli CR, Giridharan GA, Litwak KN, et al. Hemodynamic responses to continuous versus pulsatile mechanical unloading of the failing left ventricle. *ASAIO J* 2010;56:410–6.
14. Nakata K, Shiono M, Orime Y, et al. Effect of pulsatile and nonpulsatile assist on heart and kidney microcirculation with cardiogenic shock. *Artif Organs* 1996;20:681–4.
15. Nakamura T, Hayashi K, Seki J, et al. Effect of drive mode of left ventricular assist device on the left ventricular mechanics. *Artif Organs* 1988;12:56–66.
16. Hata M, Shiono M, Orime Y, et al. Coronary microcirculation during left heart bypass with a centrifugal pump. *Artif Organs* 1996;20:678–80.
17. Yamazaki K, Saito S, Kihara S, Tagusari O, Kurosawa H. Completely pulsatile high flow circulatory support with a constant-speed centrifugal blood pump: mechanisms and early clinical observations. *Gen Thorac Cardiovasc Surg* 2007;55:158–62.
18. Voitl P, Vollkron M, Bergmeister H, Wieselthaler G, Schima H. Coronary hemodynamics and myocardial oxygen consumption during support with rotary blood pumps. *Artif Organs* 2009;33:77–80.
19. Suga H, Hisano R, Hirata S, Hayashi T, Ninomiya I. Mechanism of higher oxygen consumption rate: pressure-loaded vs. Volume-loaded heart. *Am J Physiol* 1982;242:H942–8.
20. Altman JD, Kinn J, Duncker DJ, Bache RJ. Effect of inhibition of nitric oxide formation on coronary blood flow during exercise in the dog. *Cardiovasc Res* 1994;28:119–24.
21. Gorman MW, Rooke GA, Savage MV, Jayasekara MP, Jacobson KA, Feigl EO. Adenine nucleotide control of coronary blood flow during exercise. *Am J Physiol Heart Circ Physiol* 2010;299:H1981–9.
22. Tune JD, Richmond KN, Gorman MW, Feigl EO. Control of coronary blood flow during exercise. *Exp Biol Med (Maywood)* 2002;227:238–50.
23. Elhabyan AK, Reyes BJ, Hallak O, et al. Subendocardial ischemia without coronary artery disease: is elevated left ventricular end diastolic pressure the culprit? *Curr Med Res Opin* 2004;20:773–7.

厚生労働科学研究費補助金

難病・がん等の疾患分野の医療の実用化研究事業

Bridge to Decision を目的とした超小型補助循環システム並びに頭蓋内・心血管治療用の新規多孔化薄膜カバードステントに関する医師主導型治験及び実用化研究

平成 24 年度総括・分担研究報告書

研究代表者　　峰松　一夫

平成 25　(2013)年　　5 月

ACCOUNTS
of chemical research

Hyperbranched Polymeric "Star Vectors" for Effective DNA or siRNA Delivery

YASUHIDE NAKAYAMA*

Division of Medical Engineering and Materials, National Cerebral and Cardiovascular Center Research Institute

RECEIVED ON AUGUST 24, 2011

CONSPECTUS

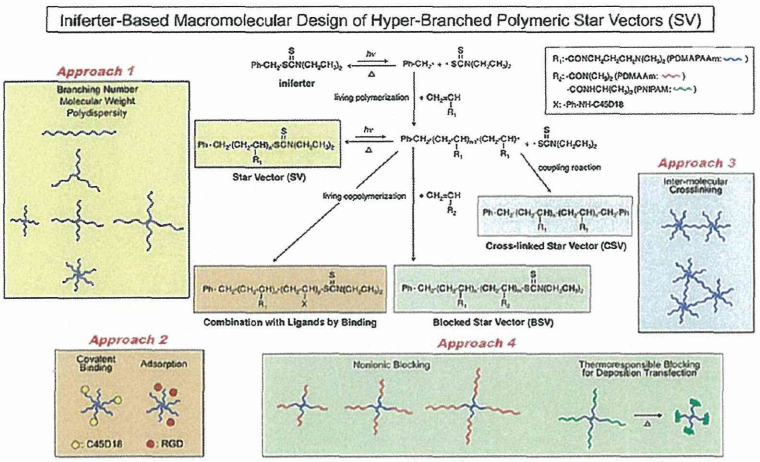

Although gene therapy offers an attractive strategy for treating inherited disorders, current techniques using viral and nonviral delivery systems have not yielded many successful results in clinical trials. Viral vectors such as retroviruses, lentiviruses, and adenoviruses deliver genes efficiently; however, the possibility of negative outcomes from viral transformation cannot be completely ruled out. In contrast, various types of nonviral vectors are attracting considerable attention because they are easier to handle and induce weak immune responses.

Cationic polymers, such as polyethylenimine (PEI) and poly(N,N-dimethylaminopropyl acrylamide) (PDMAPAAm), can generate nanoparticles through the formation of polyion complexes, "polyplexes" with DNA. These nonviral systems offer many advantages over viral systems. The primary obstacle to implementing these cationic polymers in an effective gene therapy remains their comparatively inefficient gene transfection in vivo.

We describe four strategies for the development of hyperbranched star vectors (SVs) for enhancing DNA or siRNA delivery. The molecular design was performed by living radical polymerization in which the chain length can be controlled by photoirradiation and solution conditions, including concentrations of the monomer or iniferter (a molecule that serves as a combination of initiator, transfer agent, and terminator). The branch composition is controlled by the types of monomers that are added stepwise. In our first strategy, we prepared a series of only cationic PDMAPAAm-based SVs with no branches or 3, 4, or 6 branching numbers. These SVs could form polyion complexes (polyplexes) by mixing with DNA only in aqueous solution. The relative gene expression activity of the delivered DNA increased according to the degree of branching. In addition, increasing the molecular weight of SVs and narrowing their polydispersity index (PDI) improved their activity. For targeting DNA delivery to the specific cells, we modified the SV with ligands. Interestingly, the SV could adsorb the RGD peptide, making gene transfer possible in endothelial cells which are usually refractory to such treatments. The peptide was added to the polyplex solution without covalent derivatization to the SV. The introduction of additional branching by cross-linking using iniferter-induced coupling reactions further improved gene transfection activity. After block copolymerization of PDMAPAAm-based SVs with a nonionic monomer (DMAAm), the blocked SVs (BSVs) produced polyplexes with DNA that had excellent colloidal stability for 1 month, leading to efficient in vitro and in vivo gene delivery. Moreover, BSVs served as carriers for siRNA delivery. BSVs enhanced siRNA-mediated gene silencing in mouse liver and lung. As an alternative approach, we developed a novel gene transfection method in which the polyplexes were kept in contact with their deposition surface by thermoresponsive blocking of the SV. This strategy was more effective than reverse transfection and the conventional transfection methods in solution.

Published on the Web 02/21/2012 www.pubs.acs.org/accounts
10.1021/ar200220t